Published in final edited form as:
Cytoskeleton (Hoboken). 2012 January ; 69(1): 22–32. doi:10.1002/cm.20539.

Loss of ASP but not ROPN1 reduces mammalian ciliary motility

Sarah E. Fiedler[1], **Joseph H. Sisson**[2], **Todd A. Wyatt**[2], **Jacqueline A. Pavlik**[2], **Todd M. Gambling**[3], **Johnny L. Carson**[3,4], and **Daniel W. Carr**[1,*]

[1]VA Medical Center, 3710 SW US Veterans' Hospital Rd., Portland, OR 97239; and Department of Medicine, Oregon Health & Science University, Portland, OR

[2]University of Nebraska Medical Center, Pulmonary, Critical Care, Sleep & Allergy Division, Department of Internal Medicine, Durham Research Center II 1046, 985910 Nebraska Medical Center, Omaha, NE 68198-5910

[3]Center for Environmental Medicine, Asthma, and Lung Biology, The University of North Carolina at Chapel Hill, Chapel Hill, NC 27599-7310

[4]Department of Pediatrics, The University of North Carolina at Chapel Hill, Chapel Hill, NC 27599-7220

Abstract

Protein kinase A (PKA) signaling is targeted by interactions with A-kinase anchoring proteins (AKAPs) via a dimerization/docking domain on the regulatory (R) subunit of PKA. Four other mammalian proteins (ASP, ROPN1, SP17, and CABYR) share this highly conserved RII dimerization/docking (R2D2) domain. ASP and ROPN1 are 41% identical in sequence, interact with a variety of AKAPs in a manner similar to PKA, and are expressed in ciliated and flagellated human cells. To test the hypothesis that these proteins regulate motility, we developed mutant mouse lines lacking ASP or ROPN1. Both mutant lines produced normal numbers of cilia with intact ciliary ultrastructure. Lack of ROPN1 had no effect on ciliary motility. However, the beat frequency of cilia from mice lacking ASP is significantly slower than wild type, indicating that ASP signaling may regulate ciliary motility. This is the first demonstration of in vivo function for ASP. Similar localization of ASP in mice and humans indicates that these findings may translate to human physiology, and that these mice will be an excellent model for future studies related to the pathogenesis of human disease.

Keywords

ROPN1L; ropporin; AKAP; OmniBank®

Introduction

Cilia are tiny hair-like projections that extend from the surface of almost all cell types of the human body (Inglis et al. 2006). Eukaryotic flagella share the 9+2 structure of the motile ciliary axoneme and are thus presumed to also share regulatory pathways that affect the mechanics of motility. Motile cilia/flagella function to remove debris from the respiratory tract, circulate cerebrospinal, fallopian tube and epididymal fluids, and propel spermatozoa through the female reproductive tract. Dysfunctional cilia may result in impaired respiratory function, hydrocephalus, and reduced fertility. Mammalian cilia modulate the size and shape

*Correspondence: Portland Veterans Affairs Medical Center, Mail Code R&D8, 3710 SW US Veterans Hospital Road, Portland, OR 97239. Phone: 503-721-7918; FAX: 503-721-1082; carrd@ohsu.edu.

of axonemal bend (waveform) by means of inner dynein arms and their frequency (ciliary beat frequency, CBF) by means of outer dynein arms in the axoneme (Chilvers et al. 2003; de Iongh and Rutland 1995). However, the molecular mechanisms that regulate dynein mechanics are poorly understood (Gaillard et al. 2006a).

Motile mammalian cilia and flagella alter their beat frequency in response to external signals. It is thought that ciliary dynein arms are capable of moving microtubules with either a slow or fast duty cycle. The mechanism of switching the dyneins from slow to fast is not completely understood, but both axonemal phosphorylation and dephosphorylation events of dynein light chains as well as influences on the dynein itself seem to be responsible (Salathe 2007). Numerous studies have implicated cAMP-dependent protein kinase (PKA) as a key regulatory enzyme controlling CBF (Di Benedetto et al. 1991; Hamasaki et al. 1991; Tamaoki et al. 1989; Wyatt et al. 1998). PKA is a multifunctional enzyme that is anchored to specific substrates and cellular compartments via interaction between the dimerization/docking domain on the regulatory (R) subunits of PKA and an amphipathic helix binding motif located within A-kinase anchoring proteins (AKAPs) (Fig 1A). Tethering of inactive PKA holoenzymes to specific compartments by AKAPs allows PKA to be immediately available to phosphorylate localized and/or AKAP-bound substrates in response to cAMP activation (Carr et al. 1991; Wong and Scott 2004).

Recently, four other proteins that contain the RII dimerization/docking (R2D2) domain have been identified: ROPN1 (ropporin 1), ASP (genomic name *Ropn1l*, for ROPN1-like protein), CABYR, and SP17 (Fig 1B). Based on binding studies and mutational analysis, two of these proteins (ROPN1 and ASP) appear to interact with AKAPs in a manner similar to PKA (Newell et al. 2008). ROPN1/ASP orthologs are conserved in a variety of species of animals including chickens, xenopus, fish, sea urchin, and ciliated protists, suggesting these proteins serve a vital function. These proteins do not bind cAMP; outside the docking groove, they bear little or no similarity to PKA and they do not appear to have any intrinsic enzyme activity, indicating that they have different functions than PKA (Newell et al. 2008). However, the shared R2D2 domain raises the possibility that R2D2 proteins influence AKAP-directed PKA signaling mechanisms to participate in regulation of CBF.

The flagellated protist *Chlamydomonas reinhardtii* is an important model organism in the study of ciliary/flagellar motility; its relatively simple (and completely sequenced) genome and the availability of well characterized mutants in combination with the highly conserved nature of eukaryotic ciliary structure and function allow for elegant studies that have provided many insights into the workings of cilia and cell motility (Gaillard et al. 2001; Gaillard et al. 2006b; Hasegawa et al. 1987; Hendrickson et al. 2004; Howard et al. 1994; Yang and Yang 2006; Yang et al. 2006). However, of key interest to these studies, active PKA slows dynein motors and inhibits flagellar beating in *Chlamydomonas* (Hasegawa et al. 1987; Howard et al. 1994). In contrast, beat frequency in mammalian spermatozoa and in ciliated airway tissues is stimulated in response to increases in cAMP concentrations, and addition of PKA inhibitors blocks this motility stimulation (Wyatt et al. 1998). These opposing effects of PKA activity on motility suggest that in spite of the remarkable structural and functional conservation of motile cilia/flagella, regulation of axonemal beating may differ from species to species.

Though there is a body of *in vitro* data concerning the interactions of mammalian R2D2 proteins, less has been accomplished in defining *in vivo* function, particularly for ASP and ROPN1 (Carr et al. 2001; Carr and Newell 2007; Fiedler et al. 2008; Frayne and Hall 2002; Fujita et al. 2000; Naaby-Hansen et al. 2002; Newell et al. 2008). Two observations suggest that R2D2 proteins regulate ciliary/flagellar motility: 1) adding peptides that disrupt interactions between PKA/R2D2 proteins and all cellular AKAPs (Ht31, see Fig 1A) results

in arrested bovine sperm motility, while PKA inhibitor H-89 has only a minor effect on motility and 2) *Chlamydomonas reinhardtii* mutants lacking (R2D2 protein) RSP11 have normal flagellar structure but exhibit impaired flagellar motility (Vijayaraghavan et al. 1997; Yang and Yang 2006). In the present study we created two mutant mouse lines lacking either ASP or ROPN1 to test the hypothesis that these R2D2 proteins regulate ciliary beating.

Results

R2D2 protein expression in gene trapped mice

Gene trapping is a high-throughput method of creating murine embryonic stem (ES) cell lines containing insertional mutations in genes for the purpose of generating knockout mouse strains for research in functional genomics (Zambrowicz et al. 1998). Through Lexicon Pharmaceuticals (The Woodlands, TX) and University of Michigan services, we produced two mutant mouse lines – one containing a homozygous insertional mutation in *Asp* (*Asp*^{GT} mice) and a second containing a homozygous insertional mutation in *Ropn1* (*Ropn1*^{GT} mice) (Fig. 2). These mutations disrupt expression at the protein level. Gross examination and comparative dissection of wild type, *Asp*^{GT}, and *Ropn1*^{GT} F2 mice revealed no physical defects, and both lines of mutant mice appear behaviorally normal and healthy (excluding fertility testing, which is discussed in detail below).

ASP and ROPN1 are highly expressed in testes compared to other tissues (Newell et al. 2008). Therefore, to confirm that protein expression had been inhibited in *Asp*^{GT} and *Ropn1*^{GT} mice (respectively), we performed ASP and ROPN1 western blots using testes lysates (Fig 3). ASP expression is greatly reduced in *A*^{GT} testes (compare lanes 1 and 2 of upper panel), but a longer exposure of the blot reveals that there is a very small amount (less than 2%, quantitation using NIH image) of ASP being produced (Fig S1). This hypomorphic condition was confirmed by Lexicon as a rare complication in their gene trapping method. Though not a complete knock-out, with greater than 98% reduction in ASP expression, it is a very strong knock-down. ROPN1 expression was eliminated in testes of *R*^{GT} animals (lane 3, middle panel). Because ASP and ROPN1 are both R2D2 proteins whose sequences are 39% identical, we anticipated that they might compensate for each other in their opposing gene trap animals. This supposition was supported by an increase in ROPN1 expression in *A*^{GT} testes (Fig 3, middle panel, compare lanes 1 and 2). In wild type testes, ASP is expressed in pachytene spermatocytes, similar to axonemal proteins such as dynein and radial spoke proteins [expression data from MRG (Mammalian Reproductive Genetics) database at http://mrg.genetics.washington.edu/], suggesting that ROPN1 may compensate for a sperm development function of ASP. Finally, AKAP3 western blots demonstrate equal protein loading (Fig 3, lower panel).

ASP and ROPN1 are expressed in ciliated mouse cells, and do not appear to compensate in opposing mutant tracheal tissue

We have previously shown that both ASP and ROPN1 are expressed in the ciliated cells of human bronchus (Newell et al. 2008). Human and murine ASP/ROPN1 sequences are highly conserved; ASP is 74% identical and 10% similar to human, and ROPN1 83% identical and 9% similar. In order to determine whether ASP and ROPN1 are expressed similarly in human and mouse tissue, and further to determine expression levels in our mutant mice, we harvested and fixed tracheas from wild type (WT), *Asp*^{GT} (*A*^{GT}), and *Ropn1*^{GT} (*R*^{GT}) mice in formalin, embedded the tissues in paraffin, sectioned, and stained with rabbit polyclonal antibodies against ASP and ROPN1. Consistent with localization in human trachea (Newell et al. 2008), ASP stains the cilia in wild type mouse trachea (Fig 4A left panel, arrow points to cilia), and ROPN1 stains the cytoplasm of the cilia-supporting

epithelial cells (but not the cilium itself, Fig 4B, left panel). ASP and ROPN1 staining is absent in *Asp*^{GT} and *Ropn1*^{GT} mutant tracheas, respectively [Fig 4A and B; compare WT (left panel) to *A*^{GT} (middle panel) in A, WT to and *R*^{GT} (right panel) in B].

In testes, increased expression of ROPN1 in *Asp*^{GT} testes is visible by western blot (Fig 3). However, because of the very limited number of cilia in mouse trachea and the difficulty in isolating these ciliated cells from surrounding tissue, immunohistochemical detection of ciliary proteins is preferred to western blotting techniques. Fortunately, increased ROPN1 expression in *Asp*^{GT} testes by western blot (Fig 3) is mirrored by increased intensity of DAB (brown) staining of testicular sections (data not shown). Therefore, we used our IHC staining (with careful control of variability – see Materials and Methods section for description) to determine whether ASP and/or ROPN1 cross compensate in the ciliated cells of mutant mouse trachea. In contrast to data from testes, neither ASP nor ROPN1 show a significant increase of expression or a change in staining location (i.e. ROPN1 does not stain the cilia in the absence of ASP in *Asp*^{GT} trachea) in the opposing mutant [Fig 4A and B, respectively; compare WT (left panel) to *R*^{GT} (right panel) in A, and WT (left panel) to *A*^{GT} (middle panel) in B]. Collectively, these data suggest that ASP and ROPN1 do not compensate for each other in the ciliated cells of the trachea.

Ciliogenesis, cilia alignment, and ciliary structure are normal in mice that lack *ASP* and *ROPN1*

Since ASP and ROPN1 are expressed in ciliated cells, it is possible they play roles in the development and/or maintenance of cilia. In order to determine whether ASP or ROPN1 expression is required for normal ciliary development, alignment or structural integrity, and to further confirm that there is no cross-compensation between these proteins in the ciliated cells of the trachea of *Asp*^{GT} and *Ropn1*^{GT} mice, we cross bred these two mutant lines to produce mice that are homozygous for the gene trap mutations in both *Asp* and *Ropn1,* and therefore express neither protein. As with single mutant mice, gross physical examination of these animals (*Asp*^{GT}/*Ropn1*^{GT}) reveals no abnormalities. To assess ciliogenesis, alignment and ciliary structure in the absence of ASP and ROPN1, tracheas were harvested from wild type (WT), *Asp*^{GT}, *Ropn1*^{GT} and *Asp*^{GT}/*Ropn1*^{GT} (*A*^{GT}/*R*^{GT}) mice. Tissues were fixed, embedded, sectioned and H&E stained. No differences are evident between wild type and double mutant trachea (Fig 5, arrows point to cilia; number of cilia, length of cilia, and gross morphology are all comparable), implying that neither ASP nor ROPN1 are necessary for ciliogenesis.

To determine whether there were defects in the ultrastructure or alignment of cilia not visible by light microscopy, we analyzed tracheal cilia from WT, *Asp*^{GT}, *Ropn1*^{GT}, and *Asp*^{GT}/*Ropn1*^{GT} mice with transmission electron microscopy. Cilia in mice lacking ASP and/or ROPN1 appear to be properly aligned (Fig 6A and B, note that lines corresponding to central pair angle are roughly aligned in parallel in all cases) and structurally intact (Fig 6C), including the retention of a normal central pair apparatus in flagellar axonemes that lack ASP (Fig 6D). Comparison of the percent standard deviation of central pair angles confirms that cilia from all mutant lines retain normal orientation (Table II, values of 10–15% are considered normal in clinical diagnostics, while 20–25% would suggest primary ciliary dyskinesia with disorientation (Bush et al. 1998)). Together, these data suggest that ASP and ROPN1 are not essential for establishing or maintaining ciliary orientation or structural integrity.

Lack of *ASP* results in impaired ciliary function

The localization of ASP and ROPN1 in flagellated and ciliated cells, (particularly of ASP in the motile cilia itself) and the lack of a function in ciliary development, alignment or

structural integrity suggests that R2D2 proteins may be involved in signaling events, perhaps related to motility regulation. To assess whether cilia function is altered in the absence of ASP or ROPN1, we measured cilia beat frequency in the trachea from each of our mouse lines by SAVA. When ASP is absent, basal motility is significantly reduced by about 17% [Fig. 7, compare wild type to A^{GT} and A^{GT}/R^{GT} control (CON) bars]. In all lines, stimulation with procaterol (PRO, a beta-adrenergic receptor agonist) significantly increases CBF (Fig. 7, compare PRO bars), providing additional evidence that cilia are structurally intact in mice lacking these proteins. Of note, the reduction in basal CBF is no greater in double mutant cilia (A^{GT}/R^{GT}) than the single mutant Asp^{GT}, and there is no reduction in the basal motility of $Ropn1^{GT}$ cilia, suggesting that ASP, but not ROPN1, functions as a key molecule in the maintenance of basal ciliary beat frequency. In combination with immunohistochemistry (Fig 4), these data also indicate that ROPN1 does not compensate for ASP in ciliated cells, and thus ASP plays a unique role in ciliary motility.

Lack of ROPN1 impairs sperm motility and male fertility, while lack of ASP alone does not significantly affect sperm function

Because motile mammalian cilia and sperm flagella both contain a central 9+2 axoneme, they also likely to share some mechanisms of motility regulation. However, mammalian spermatozoa also contain the unique structures of the outer dense fibers and the fibrous sheath surrounding the axoneme, and therefore also have the potential for regulatory mechanisms not found in cilia. To assess motility, caudal epididymal sperm were observed by a trained observer in a warm 96-well plate under a light microscope. All mutant mouse lines (Asp^{GT}, $Ropn1^{GT}$ and $Asp^{GT}/Ropn1^{GT}$) produced normal numbers of mature sperm (i.e. count did not differ significantly from wild type counts, data not shown). However, under conditions which supported vigorous motility of wild type and Asp^{GT} sperm, $Ropn1^{GT}$ sperm displayed motility that varied from slightly less vigorous than wild type (some progressive) to nearly immotile (only sluggish, twitching movement with no progression). Sperm from double mutant ($Asp^{GT}/Ropn1^{GT}$) animals are completely immotile (Table I). To determine whether this reduction in motility affected fertility, ten mature male mice from each line (wild type, Asp^{GT}, $Ropn1^{GT}$ and $Asp^{GT}/Ropn1^{GT}$) were housed with wild type female animals for a minimum of five weeks. Consistent with motility observations, Asp^{GT} mice exhibit normal fertility, while $Ropn1^{GT}$ mice are subfertile (fewer litters, with significantly fewer pups per litter) and $Asp^{GT}/Ropn1^{GT}$ mice are infertile, (Table I); presence of copulatory plugs in females paired with $Asp^{GT}/Ropn1^{GT}$ males confirmed mating and necropsy revealed no pregnancy failure, indicating that infertility is likely due to lack of fertilization.

Analyses of hypomorphic compensation

Because of the hypomorphic condition of the Asp^{GT} mice, we also investigated whether the small amount of ASP expressed in these mice is upregulated in either the testes or tracheal cilia of double mutant animals ($Asp^{GT}/Ropn1^{GT}$). Western blots indicate that there may be a slight increase in ASP expression in the testes of $Asp^{GT}/Ropn1^{GT}$ compared to Asp^{GT} single mutant mice (Figure S2A), however, IHC staining of trachea indicates that there is no upregulation of ASP expression the double mutant ($Asp^{GT}/Ropn1^{GT}$) mice in comparison to Asp^{GT} ciliated cells (Figure S2B).

Discussion

We originally identified ASP and ROPN1 in a yeast-two hybrid screen looking for AKAP3 binding partners in testes, and have since determined that both ASP and ROPN1 bind a variety of AKAPs via a conserved R2D2 domain, but, until now, no *in vivo* role for these proteins had been identified (Newell et al. 2008). Because these proteins interact with

AKAPs via the PKA binding site, defining their functions separate from PKA signaling is especially complex. Therefore, we reasoned the best way to determine function was production of mice that lacked ASP and/or ROPN1. Our previous studies have shown that ASP is predominantly located in motile cilia while ROPN1 is predominantly located in sperm flagellum (Newell et al. 2008). In the present study we created mutant mouse lines lacking either ASP or ROPN1; offspring from these mice appeared healthy, and examination of tissues and cells that normally express ASP and ROPN1 [testes/sperm and trachea/ciliated cells] revealed no gross developmental or structural abnormalities. However, we cannot entirely rule out the possibility that the very small amount of ASP still being produced is sufficient to maintain normal development/structure in Asp^{GT} cilia and flagella. The slight upregulation of (hypomorphic) ASP expression in the testes (but not in the trachea) of double mutant ($Asp^{GT}/Ropn1^{GT}$) animals may hint that ASP plays such a role in testes, but this cannot be determined with any certainty at present.

Chlamydomonas mutants that lack R2D2 protein RSP11 have normal flagellar structure, but exhibit impaired motility (Yang and Yang 2006). This observation, coupled with the localization of ASP and ROPN1 in ciliated/flagellated cells, and the lack of a developmental, structural, or disorientation phenotype in our single mutant animals led us to hypothesize that ASP and/or ROPN1 may function to regulate motility. We thus examined tracheal cilia and indeed determined that lack of ASP results in impaired motility. $Asp^{-/-}$ mice exhibit reduced basal ciliary motility; statistically significant reductions of this magnitude (approximately 17%) have been shown to be biologically important as even a 2 Hz decrease in cilia beating results in a significant reduction in *in vivo* bacterial clearance (Vander Top et al. 2005). In contrast, lack of ROPN1 had no effect on CBF; this result is perhaps not unexpected due to the exclusion of ROPN1 from the cilia itself and its failure to relocalize in A^{GT} cilia. In combination with EM data indicating that $Asp^{GT}/Ropn1^{GT}$ cilia are structurally intact and properly oriented, these data suggest that ASP (but not ROPN1) functions as a critical, non-redundant regulator of ciliary motility in mammalian cells. Further, since CBF is thought to be modulated by the outer dynein arms (ODA) in the axoneme, ASP may thus participate in signaling pathways that affect ODA function.

While lack of ROPN1 has no effect on cilia beat frequency, sperm from $Ropn1^{GT}$ mice do exhibit altered motility, and these males are subfertile, producing fewer and smaller litters. Strikingly, mice that lack both ASP and ROPN1 ($Asp^{GT}/Ropn1^{GT}$) are infertile due to sperm immotility. While testes development and testicular spermatogenesis appears normal in these mice, mature sperm have significant structural defects in the principal piece of the flagellum; our current analyses indicate that the axonemes of these sperm are intact, but that the sperm-specific structure of the fibrous sheath (FS) (where ROPN1 is expressed in wild type sperm) is disrupted (Fujita et al. 2000). Additionally, our data suggest that though ASP does not appear to have an irreplaceable role in sperm motility or fertility (as indicated by the normal fertility parameters exhibited by Asp^{GT} mice presented in Table I), it may compensate for ROPN1 in $Ropn1^{GT}$ sperm acting to preserve the structural integrity of the FS, perhaps via AKAP interactions. Further studies into the function of ROPN1 in sperm integrity, motility and fertility are ongoing.

Data presented here indicate that ASP plays a role in ciliary motility, perhaps via regulation of axonemal signaling. We have previously demonstrated that ASP binds a variety of AKAPs, which raises the possibility that AKAP interactions are part of a mechanism by which ASP affects ciliary beat frequency. Two AKAPs have been identified in mammalian ciliary axonemes: AKAP28 and radial spoke protein 3 (RSP3). In *Chlamydomonas*, RSP3 forms a homodimer that is located at the base of the spoke stalk domain in the axoneme and is thus in position to mediate the anchoring of PKA or AKAP-binding proteins to control dynein activity and thus ciliary beating (Wirschell et al. 2008). Studies employing site-

directed mutagenesis of the RSP3 gene in the region coding for the PKA binding site suggest that RSP3 is an AKAP required for regulation of axonemal PKA and regulation of flagellar bending by the radial spokes, as these mutants exhibit abnormal flagellar motility (Gaillard et al. 2006b). The fact that R2D2 proteins share an AKAP binding site with the regulatory subunit of PKA suggests that they may compete with PKA *in vivo* for binding to mammalian AKAPs, thus controlling the amount of PKA bound to any particular AKAP at any given time. Controlling PKA/AKAP interaction would regulate the ability of PKA to act on key substrates that may be essential for modifying CBF. We know that both PKA and R2D2 proteins strongly interact with AKAPs *in vitro*, but *in vivo* associations are less well defined for PKA, and absent for ASP. One mechanism by which AKAP interactions are known to be modulated is via changing binding affinities due to phosphorylation of the AKAP (Fiedler et al. 2008). Relevant to these studies, it has recently been demonstrated that both ERK1/2 and PKA can phosphorylate RSP3 in a transfected mammalian cell line, and that phosphorylation modulates PKA binding (Jivan et al. 2009). We have previously determined that both recombinant and endogenously expressed ASP and PKA (from mouse testes) interact with human recombinant RSP3 (Newell et al. 2008). Further studies will test the hypothesis that phosphorylation of RSP3 differentially modifies its affinity for ASP and PKA.

In addition to RSP3, the only other human ciliary axonemal AKAP that has been identified to date is AKAP28 (Kultgen et al. 2002). While we speculate herein that AKAPs have changing binding affinities for PKA and R2D2 proteins based on dynamic post-translational modifications such as phosphorylation, an alternate hypothesis is that AKAP28 and RSP3 each interact with a unique subset of binding proteins – perhaps one AKAP with PKA and the other with ASP. We believe that both AKAP28 and RSP3 will prove to be players in ciliary beat regulation along with PKA and ASP, and future studies will seek to identify *in vivo* post-translational modifications on AKAPs, and what effect these modifications have on PKA versus ASP binding affinity.

Outside the dimerization/docking domain, there is very little sequence homology between the regulatory subunits of PKA and the R2D2 proteins, thus these proteins are not likely to interact with the catalytic subunits of PKA. We have also demonstrated that none of the R2D2 proteins bind cAMP (Newell et al. 2008). Sequence analysis indicates that none of these proteins appears to contain intrinsic enzyme activity. Based on these data, we speculate that in addition to participating in PKA regulation via competitive AKAP-binding, R2D2 proteins may also prove to function in a manner similar to the regulatory subunit of PKA — that is, they coordinate signaling events by simultaneously binding not only to AKAPs, but also to one or more signaling molecules. Therefore we predict that, similar to RII, ASP binds to a signaling enzyme and serves as a regulatory subunit (as does RII for PKA), modulating the activity of whatever kinase or phosphatase it interacts with. We speculate that PKC would be a good candidate enzyme for regulation by ASP as lack of ASP results in decreased ciliary motility and it is known that activation of PKC decreases CBF (Salathe 2007; Salathe et al. 1993; Slager et al. 2008). Studies are underway to examine PKC activity in Asp^{GT} mice.

Mucociliary clearance is an essential part of the innate defense of the respiratory membranes, airway and lungs from inhaled allergens, pathogens, toxins and pollutants (Mall 2008; Stannard and O'Callaghan 2006). In humans, impaired ciliary function can have many negative health consequences; respiratory diseases such as primary ciliary dyskinesia, cystic fibrosis, asthma and chronic obstructive pulmonary disease (COPD) are associated with defects in mucociliary clearance. In many of these diseases, underlying genetic defects in cilia are suspected, though identification of specific mutations and complete understanding of etiology and pathogenesis are largely elusive (Livraghi and Randell 2007).

Interestingly, though CBF is decreased in mice that lack ASP, motility can be stimulated (with procaterol, a β agonist), providing further evidence that the cilia in these mice are structurally intact. The vast majority of mouse models that display abnormal ciliary motility have incomplete structures (and missing proteins) within the cilia, often within the axoneme. Because cilia are signaling antennae as well as mechanical removers of pathogens and pollutants, these structural defects may make it difficult to isolate the effects of altered signaling events versus reduced mechanical function. Additionally, genetically engineered mice with primary cilia disorders develop hydrocephalus internus during early brain development. Due to the high and early mortality related to hydrocephalus formation, a detailed analysis of the pulmonary phenotype has been difficult in these mice (Brody et al. 2000). The phenotype of our Asp^{GT} mice, in which CBF is reduced without an associated structural defect or early death of the animals, provides a rare opportunity to determine the contribution of normal ciliary motility to the mucociliary clearance apparatus, and how its impairment might contribute to the development of ciliopathies and diseases of compromised mucociliary clearance. We show herein that the expression pattern of ASP and ROPN1 in ciliated airway cells of humans and mice is comparable and sequence identity is high, making our mutant mice excellent candidates as models for future studies of the role of R2D2 proteins in human airway function, and the role of dysfunctional ciliary motility in the etiology and pathogenesis of disease.

Materials and Methods

Chemical sources

Unless otherwise noted, all chemicals were obtained from Sigma-Aldrich (St. Louis, MO).

Production and breeding of mice

These studies were approved by the Portland Veterans' Affairs Medical Center (PVAMC) IACUC, which follows the guidelines of the Office of Laboratory Animal Welfare (OLAW) and sets policies according to the *Guide for the Care and Use of Laboratory Animals* and the *Department of Veterans Affairs Handbook 1200.7, Use of Animals in Research*. Mice were housed at the PVAMC Veterinary Medical Unit. Mice used in these experiments had reached sexual maturity (at least 6 weeks of age), and all were euthanized by CO_2 asphyxiation.

Mutant mouse lines that contain insertional mutations in *Asp* and *Ropn1* that interrupt protein expression were purchased from Lexicon Pharmaceuticals (The Woodlands, TX) [see (Zambrowicz et al. 1998) for methodology, and Figure 2 for the genotyping schematic].

Mutant mouse genotyping

ASP accession: NM_145852

ROPN1 accession: NM_030744

Genotyping primers:

Fwd ASP: 5′-ATGAGTGATGTTGATGACTGGGTG-3′

Rev ASP: 5′-CAGAGACAGAAACGCAAGTGTGC-3′

Fwd ROPN1: 5′-GCCAATTCCAATGCAATCGC-3′

Rev ROPN1: 5′-CCCTCAGGGTCTTATGTTGAAGTCC-3′

Rev LTR: 5′-ATAAACCCTCTTGCAGTTGCATC-3′

Mouse tail biopsies were obtained at weaning; tissue was digested at 50°C 4 h to overnight in a 500 μg/ml Proteinase K buffer (5 mM EDTA, 0.5% SDS, 200 mM NaCl, 100 mM Tris-HCl, pH 8.8). Genomic DNA was precipitated by addition of isopropanol and resuspended in TE buffer. PCR was performed on a 9800 Fast Thermocycler using GeneAmp Fast PCR Mix (both Applied Biosystems, Foster City, CA). Throughout this manuscript, Asp^{GT} (or A^{GT}) refers to animals that are homozygous for the gene trap insertion in *Asp*, and $Ropn1^{GT}$ (or R^{GT}) refers to animals that are homozygous for the gene trap insertion in *Ropn1*. $Asp^{GT}/Ropn1^{GT}$ (or A^{GT}/R^{GT}) are homozygous for both gene trap insertions.

Isolation and preparation of testes for western blot

Immediately after CO_2 euthanization, testes were removed from wild type, Asp^{GT} or $Ropn1^{GT}$ mice. Testes were crushed in liquid nitrogen, lysed in lysis buffer (10 mM Tris pH 7.6, 150 mM NaCl, 1% TritonX-100, 1% deoxycholate, 0.1% SDS, 5 mM EDTA), and sonicated. The insoluble fraction was removed and SDS sample buffer was added to the supernatants. Protein concentration was determined using a SPN protein assay (G-Biosciences, Maryland Heights, MO), and equal loading (20 μg per lane) was confirmed by Coomassie stain. SDS-PAGE and western blots using rabbit polyclonal antibodies to ASP, ROPN1 and AKAP3 [antibodies characterized in (Newell et al. 2008)] were performed as previously described (Newell et al. 2008).

Immunohistochemistry

Immunohistochemical staining was performed as described previously (Newell et al. 2008) with minor modifications as follows. ROPN1 antibody was diluted 1:2000, and all primary antibody incubations were for 1 h. Pictures were taken with a Zeiss (Gottingen, Germany) AxioCam connected to an AxioPlan2 epifluorescence microscope, and images were processed in Adobe Photoshop CS2 version 9.0.2 (Adobe Systems, San Jose, CA). In order to make valid comparisons of staining between wild type and mutant animals in Fig 4, we tightly controlled for variables in staining, image capture and image processing. First, wild type, Asp^{GT} and $Ropn1^{GT}$ sections were affixed to a single slide to ensure that all three sections were stained with identical conditions. Secondly, imaging parameters on the microscope (lighting, brightness, contrast, exposure, and color balance) were set on wild type sections, then maintained for all subsequent pictures. Finally, any adjustments made in Photoshop (minor brightness/contrast modifications) were applied equally to all images.

Transmission Electron Microscopy

Tracheal rings for ultrastructural analysis were underwent primary fixation in phosphate buffered 2% glutaraldehyde + 2% paraformaldehyde supplemented with 0.5% aqueous tannic acid. The tissues were subsequently post-fixed in 1% buffered osmium tetroxide, and dehydrated through serial alchohol changes, followed by infiltration with an epoxy resin. The infiltrated tissues were polymerized and silver sections were obtained from the resultant specimen blocks and mounted on copper EM specimen grids. Sections were post-stained by standard techniques using uranyl acetate and lead citrate. Sections were viewed and photographed in a Zeiss EM 900 transmission electron microscope at an accelerating voltage of 60 kV.

Trachea harvesting, treatment and cilia beat frequency

Trachea were removed and maintained in a closed sterile 1.5 mL tubes in serum-free M199 containing penicillin/streptomycin (100 units/100 μg per mL) (Gibco, Carlsbad, CA) until processing. Tracheal rings were cut (width ≈0.5 mm) from the distal end of the trachea just

proximal to the first bifurcation of the trachea into right and left mainstream bronchi. The rings were placed in 35 mm dishes containing serum-free M199 (Gibco) for CBF determinations. Following baseline CBF determination, the rings were stimulated with procaterol at a final concentration of 1 μM. The rings and tissue were incubated for 30 min at 37°C, 5% CO_2 then allowed to equilibrate at 25°C for 10 min. The final CBF reading was taken from the tracheal rings.

The motion of the actively beating cilia on the tracheal ring was quantified using phase contrast microscopy, and computerized frequency spectrum analysis. During CBF measurement, tracheal rings were maintained at a constant temperature (24°C ± 0.5°C) by a thermostatically controlled heated stage, as the temperature gradient is known to affect CBF (Sanderson and Dirksen 1989). All observations were recorded for analysis with a Kodak Megaplus 310 analog/digital video camera (Eastman Kodak Motion Analysis Systems Division, San Diego, CA). Whole-field analysis was performed and the CBF determined by collecting data sampled at 85 fps from 256 samples (3 seconds) and performing frequency spectrum analysis using the Sisson-Ammons Video Analysis (SAVA) system (Sisson et al. 2003).

Sperm motility and male fertility analyses

To assess sperm motility, caudal epididymides were minced in a 96-well plate in Buffer A (120 mM NaCl, 10 mM KCl, 10 mM Tris pH 7.4, 10 mM glucose, 10 mg/ml bovine serum albumin) then placed in a 37°C incubator/5% CO2 for at least 15 min in order to allow sperm to swim up prior to counting. Motility was assessed on a Nikon (Melville, NY) TMS light microscope fit with a stage warmer set to 37°C by a trained observer who was blind to the genotype of the animals being assessed. To determine fertility, ten male mice from each line (wild type, homozygous Asp^{GT}, homozygous $Ropn1^{GT}$ and double homozygous $Asp^{GT}/Ropn1^{GT}$) were housed with wild type female mice for a minimum of 5 weeks. At the termination of the mating period, females were either kept for a minimum of three weeks (one gestational period) or euthanized and necropsied to ensure that all pregnancies were detected and recorded.

Statistical analysis

Ciliary central pair angles presented in Table II were measured in Photoshop CS2 Version 9.0.2, and standard deviation of angles was calculated in Microsoft Excel 2007. Analyses for Figure 7 were performed in Graphpad Prism 4 for Macintosh, Version 4.0c. Significance was determined by ANOVA.

Supplementary Material

Refer to Web version on PubMed Central for supplementary material.

Acknowledgments

The authors would like to thank Randy Baldwin for animal care work, Carolyn Gendron and Cara Poage for histology, and Drs. George Witman and Gary Olson for his helpful comments in the preparation of this manuscript.

Funding for this project is provided by NIH Grant HD 36408 (DWC), VA Merit Award (DWC), NIH Grant 5 R37AA008769-18 (JHS), a Clinical Innovator Award (JLC) from the Flight Attendant Medical Research Institute, and the US Environmental Protection Agency (JLC). Although the research described in this article has been funded wholly or in part by the US Environmental Protection Agency through cooperative agreement CR833463-01 with the Center for Environmental Medicine, Asthma, and Lung Biology at the University of North Carolina at Chapel Hill, it has not been subjected to the agency's required peer and policy review, and therefore does not necessarily reflect the views of the agency and no official endorsement should be inferred. Mention of trade names or commercial products does not constitute endorsement or recommendation for use.

References

Brody SL, Yan XH, Wuerffel MK, Song SK, Shapiro SD. Ciliogenesis and left-right axis defects in forkhead factor HFH-4-null mice. Am J Respir Cell Mol Biol. 2000; 23(1):45–51. [PubMed: 10873152]

Bush A, Cole P, Hariri M, Mackay I, Phillips G, O'Callaghan C, Wilson R, Warner JO. Primary ciliary dyskinesia: diagnosis and standards of care. Eur Respir J. 1998; 12(4):982–8. [PubMed: 9817179]

Carr DW, Fujita A, Stentz CL, Liberty GA, Olson GE, Narumiya S. Identification of sperm-specific proteins that interact with A-kinase anchoring proteins in a manner similar to the type II regulatory subunit of PKA. J Biol Chem. 2001; 276(20):17332–8. [PubMed: 11278869]

Carr DW, Newell AE. The role of A-kinase anchoring proteins (AKaps) in regulating sperm function. Soc Reprod Fertil Suppl. 2007; 63:135–41. [PubMed: 17566268]

Carr DW, Stofko-Hahn RE, Fraser ID, Bishop SM, Acott TS, Brennan RG, Scott JD. Interaction of the regulatory subunit (RII) of cAMP-dependent protein kinase with RII-anchoring proteins occurs through an amphipathic helix binding motif. J Biol Chem. 1991; 266(22):14188–92. [PubMed: 1860836]

Chilvers MA, Rutman A, O'Callaghan C. Ciliary beat pattern is associated with specific ultrastructural defects in primary ciliary dyskinesia. J Allergy Clin Immunol. 2003; 112(3):518–24. [PubMed: 13679810]

de Iongh RU, Rutland J. Ciliary defects in healthy subjects, bronchiectasis, and primary ciliary dyskinesia. Am J Respir Crit Care Med. 1995; 151(5):1559–67. [PubMed: 7735615]

Di Benedetto G, Manara-Shediac FS, Mehta A. Effect of cyclic AMP on ciliary activity of human respiratory epithelium. Eur Respir J. 1991; 4(7):789–95. [PubMed: 1659538]

Fiedler SE, Bajpai M, Carr DW. Identification and characterization of RHOA-interacting proteins in bovine spermatozoa. Biol Reprod. 2008; 78(1):184–92. [PubMed: 17928627]

Frayne J, Hall L. A re-evaluation of sperm protein 17 (Sp17) indicates a regulatory role in an A-kinase anchoring protein complex, rather than a unique role in sperm-zona pellucida binding. Reproduction. 2002; 124(6):767–74. [PubMed: 12530914]

Fujita A, Nakamura K, Kato T, Watanabe N, Ishizaki T, Kimura K, Mizoguchi A, Narumiya S. Ropporin, a sperm-specific binding protein of rhophilin, that is localized in the fibrous sheath of sperm flagella. J Cell Sci. 2000; 113 (Pt 1):103–12. [PubMed: 10591629]

Gaillard AR, Diener DR, Rosenbaum JL, Sale WS. Flagellar radial spoke protein 3 is an A-kinase anchoring protein (AKAP). J Cell Biol. 2001; 153(2):443–8. [PubMed: 11309423]

Gaillard AR, Fox LA, Rhea JM, Craige B, Sale WS. Disruption of the A-Kinase-anchoring Domain in Flagellar Radial Spoke Protein 3 Results in Unregulated Axonemal PKA Activity and Abnormal Flagellar Motility. Mol Biol Cell. 2006a

Gaillard AR, Fox LA, Rhea JM, Craige B, Sale WS. Disruption of the A-kinase anchoring domain in flagellar radial spoke protein 3 results in unregulated axonemal cAMP-dependent protein kinase activity and abnormal flagellar motility. Mol Biol Cell. 2006b; 17(6):2626–35. [PubMed: 16571668]

Hamasaki T, Barkalow K, Richmond J, Satir P. cAMP-stimulated phosphorylation of an axonemal polypeptide that copurifies with the 22S dynein arm regulates microtubule translocation velocity and swimming speed in Paramecium. Proc Natl Acad Sci U S A. 1991; 88(18):7918–22. [PubMed: 1654550]

Hasegawa E, Hayashi H, Asakura S, Kamiya R. Stimulation of in vitro motility of Chlamydomonas axonemes by inhibition of cAMP-dependent phosphorylation. Cell Motil Cytoskeleton. 1987; 8(4): 302–11. [PubMed: 2826019]

Hendrickson TW, Perrone CA, Griffin P, Wuichet K, Mueller J, Yang P, Porter ME, Sale WS. IC138 is a WD-repeat dynein intermediate chain required for light chain assembly and regulation of flagellar bending. Mol Biol Cell. 2004; 15(12):5431–42. [PubMed: 15469982]

Howard DR, Habermacher G, Glass DB, Smith EF, Sale WS. Regulation of Chlamydomonas flagellar dynein by an axonemal protein kinase. J Cell Biol. 1994; 127(6 Pt 1):1683–92. [PubMed: 7798320]

Inglis PN, Boroevich KA, Leroux MR. Piecing together a ciliome. Trends Genet. 2006; 22(9):491–500. [PubMed: 16860433]

Jivan A, Earnest S, Juang YC, Cobb MH. Radial spoke protein 3 is a mammalian protein kinase A-anchoring protein that binds ERK1/2. J Biol Chem. 2009; 284(43):29437–45. [PubMed: 19684019]

Kultgen PL, Byrd SK, Ostrowski LE, Milgram SL. Characterization of an A-kinase anchoring protein in human ciliary axonemes. Mol Biol Cell. 2002; 13(12):4156–66. [PubMed: 12475942]

Livraghi A, Randell SH. Cystic fibrosis and other respiratory diseases of impaired mucus clearance. Toxicol Pathol. 2007; 35(1):116–29. [PubMed: 17325980]

Mall MA. Role of cilia, mucus, and airway surface liquid in mucociliary dysfunction: lessons from mouse models. J Aerosol Med Pulm Drug Deliv. 2008; 21(1):13–24. [PubMed: 18518828]

Naaby-Hansen S, Mandal A, Wolkowicz MJ, Sen B, Westbrook VA, Shetty J, Coonrod SA, Klotz KL, Kim YH, Bush LA, et al. CABYR, a novel calcium-binding tyrosine phosphorylation-regulated fibrous sheath protein involved in capacitation. Dev Biol. 2002; 242(2):236–54. [PubMed: 11820818]

Newell AE, Fiedler SE, Ruan JM, Pan J, Wang PJ, Deininger J, Corless CL, Carr DW. Protein kinase A RII-like (R2D2) proteins exhibit differential localization and AKAP interaction. Cell Motil Cytoskeleton. 2008; 65(7):539–52. [PubMed: 18421703]

Salathe M. Regulation of mammalian ciliary beating. Annu Rev Physiol. 2007; 69:401–22. [PubMed: 16945069]

Salathe M, Pratt MM, Wanner A. Protein kinase C-dependent phosphorylation of a ciliary membrane protein and inhibition of ciliary beating. J Cell Sci. 1993; 106 (Pt 4):1211–20. [PubMed: 7510301]

Sanderson MJ, Dirksen ER. Mechanosensitive and beta-adrenergic control of the ciliary beat frequency of mammalian respiratory tract cells in culture. Am Rev Respir Dis. 1989; 139(2):432–40. [PubMed: 2536528]

Sisson JH, Stoner JA, Ammons BA, Wyatt TA. All-digital image capture and whole-field analysis of ciliary beat frequency. J Microsc. 2003; 211(Pt 2):103–11. [PubMed: 12887704]

Slager RE, Devasure JM, Pavlik JA, Sisson JH, Wyatt TA. RACK1, a PKC targeting protein, is exclusively localized to basal airway epithelial cells. The journal of histochemistry and cytochemistry : official journal of the Histochemistry Society. 2008; 56(1):7–14. [PubMed: 17875659]

Stannard W, O'Callaghan C. Ciliary function and the role of cilia in clearance. J Aerosol Med. 2006; 19(1):110–5. [PubMed: 16551222]

Tamaoki J, Kondo M, Takizawa T. Effect of cAMP on ciliary function in rabbit tracheal epithelial cells. J Appl Physiol. 1989; 66(3):1035–9. [PubMed: 2468639]

Vander Top EA, Wyatt TA, Gentry-Nielsen MJ. Smoke exposure exacerbates an ethanol-induced defect in mucociliary clearance of Streptococcus pneumoniae. Alcoholism, clinical and experimental research. 2005; 29(5):882–7.

Vijayaraghavan S, Goueli SA, Davey MP, Carr DW. Protein kinase A-anchoring inhibitor peptides arrest mammalian sperm motility. J Biol Chem. 1997; 272(8):4747–52. [PubMed: 9030527]

Wirschell M, Zhao F, Yang C, Yang P, Diener D, Gaillard A, Rosenbaum JL, Sale WS. Building a radial spoke: flagellar radial spoke protein 3 (RSP3) is a dimer. Cell Motil Cytoskeleton. 2008; 65(3):238–48. [PubMed: 18157907]

Wong W, Scott JD. AKAP signalling complexes: focal points in space and time. Nat Rev Mol Cell Biol. 2004; 5(12):959–70. [PubMed: 15573134]

Wyatt TA, Spurzem JR, May K, Sisson JH. Regulation of ciliary beat frequency by both PKA and PKG in bovine airway epithelial cells. Am J Physiol. 1998; 275(4 Pt 1):L827–35. [PubMed: 9755116]

Yang C, Yang P. The flagellar motility of Chlamydomonas pf25 mutant lacking an AKAP-binding protein is overtly sensitive to medium conditions. Mol Biol Cell. 2006; 17(1):227–38. [PubMed: 16267272]

Yang P, Diener DR, Yang C, Kohno T, Pazour GJ, Dienes JM, Agrin NS, King SM, Sale WS, Kamiya R, et al. Radial spoke proteins of Chlamydomonas flagella. J Cell Sci. 2006; 119(Pt 6):1165–74. [PubMed: 16507594]

Zambrowicz BP, Friedrich GA, Buxton EC, Lilleberg SL, Person C, Sands AT. Disruption and sequence identification of 2,000 genes in mouse embryonic stem cells. Nature. 1998; 392(6676): 608–11. [PubMed: 9560157]

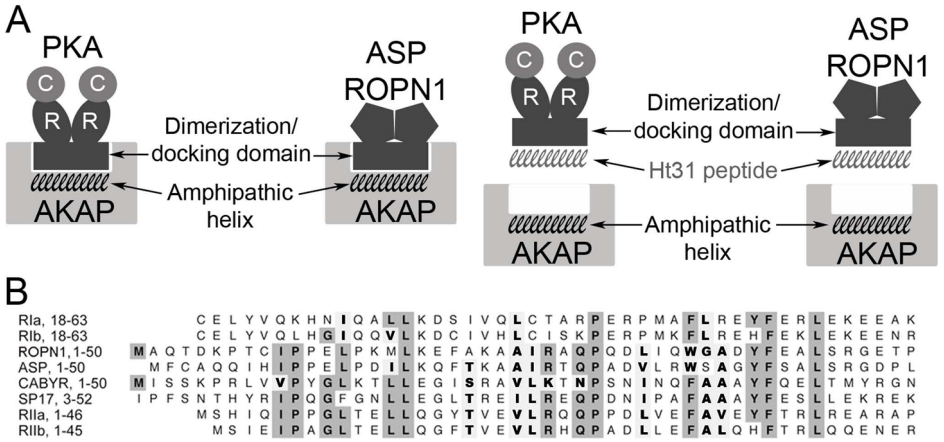

Figure 1. Model of AKAP interaction with PKA RII and RII-like (R2D2) proteins

In A, the amphipathic helix region on AKAPs interacts with the dimerization/docking (R2D2) domain of both PKA and R2D2 proteins ASP and ROPN1. This interaction is interrupted by Ht31 competitively binding to the R2D2 domains of PKA and the R2D2 proteins. In B, amino acid sequence alignment of the R2D2 domains of ROPN1, ASP, SP17, CABYR, PKA RI and RII. Gray boxes highlight conserved identity, bold letters highlight conserved similarity.

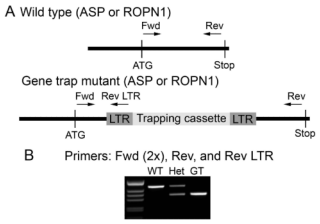

Figure 2. Genotyping scheme

A. Mutations that interrupt expression at the protein level are contained in a trapping cassette that is flanked by identical LTR (long terminal repeat) regions. This construct is inserted in to the gene of interest (ASP or ROPN1 in this case). To identify animals containing the mutation, protein-specific primers to ASP and ROPN1 were designed to lie on opposite sides of the insertion site. A reverse LTR (Rev-LTR) primer sits on the mutant construct. B. When the Rev-LTR primer is paired with the protein-specific forward (Fwd) primer, a mutation-specific product is generated by PCR (band in GT lane). Protein-specific Fwd-Rev primer pairs will only generate a visible product in a wild type allele under our PCR conditions (band in WT lane, extension time is too low to allow formation of larger product in alleles that contain the mutant construct).

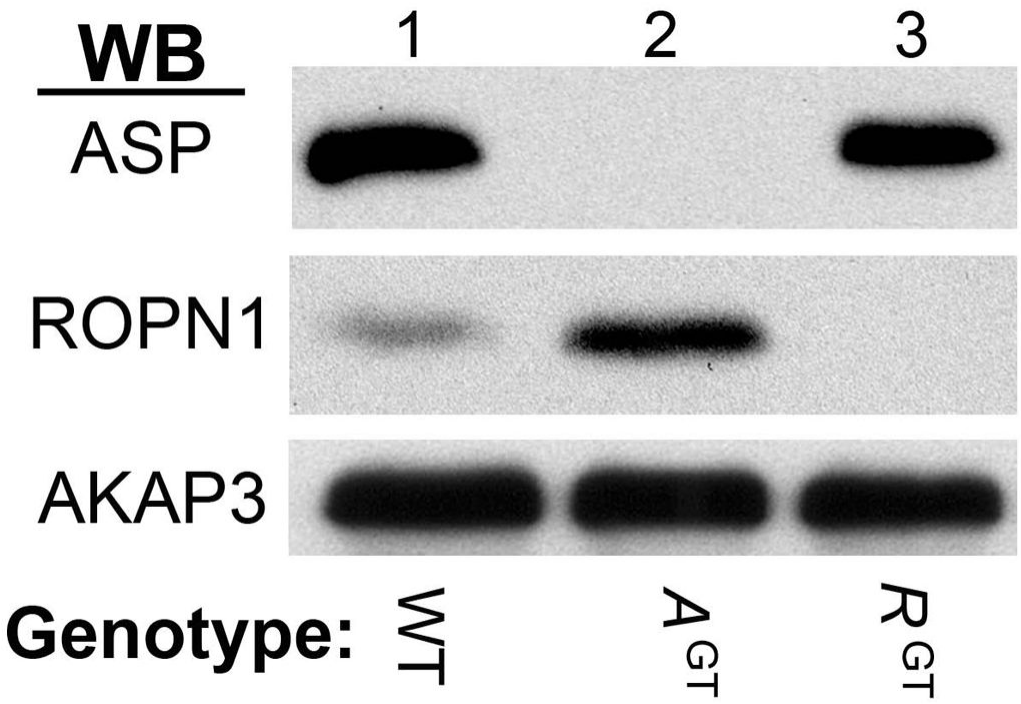

Figure 3. R2D2 protein expression in testes of mutant mice

Expression of ASP and ROPN1 from homozygous wild type (WT, lane 1), homozygous *Asp* gene trap (A^{GT}, lane 2), or homozygous *Ropn1* gene trap (R^{GT}, lane 3) mice. Western blots using rabbit polyclonal antibodies against ASP (top panel), ROPN1 (middle panel) and AKAP3 (lower panel) were performed. The western blots pictured here are representative of at least three independent experiments, on at least three unique sets of mice.

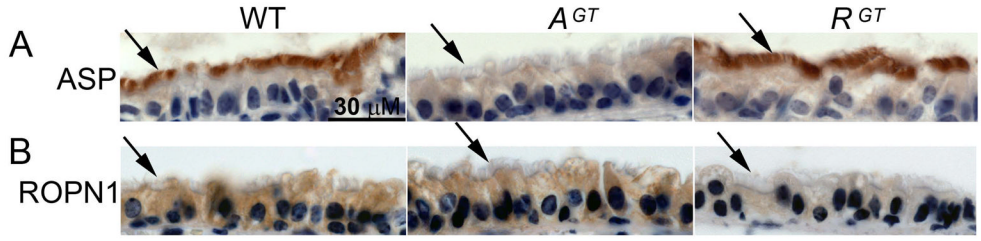

Figure 4. ASP and ROPN1 are expressed in ciliated mouse cells, and expression is knocked out in *Asp*^{GT} and *Ropn1*^{GT} trachea, respectively

Immunohistochemical staining of wild type (WT), *Asp*^{GT} (*A*^{GT}) and *Ropn1*^{GT} (*R*^{GT}) trachea sections using rabbit polyclonal antibodies to ASP (upper panels) or ROPN1 (lower panels) shows DAB positive (brown) staining. Blue hematoxylin counter-stain stains nucleic acid-rich regions. Arrows point to cilia, where ASP is expressed in WT tissue, but ROPN1 is not. These (100X oil immersion) images are representative of three independent experiments on three unique sets of mice.

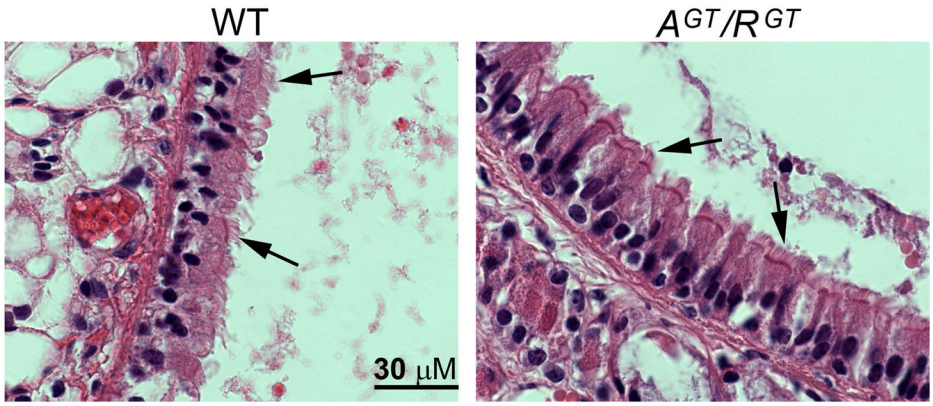

Figure 5. Ciliogenesis is normal in mice that lack both ASP and ROPN1

Trachea were harvested from wild type (WT) and *Asp*^{GT}/*Ropn1*^{GT} (A^{GT}/R^{GT}) mice, fixed in formalin, embedded in paraffin, sectioned, and H&E stained. Images are 100X oil immersion. Arrows point to cilia. These images are representative of three independent experiments on three unique sets of mice.

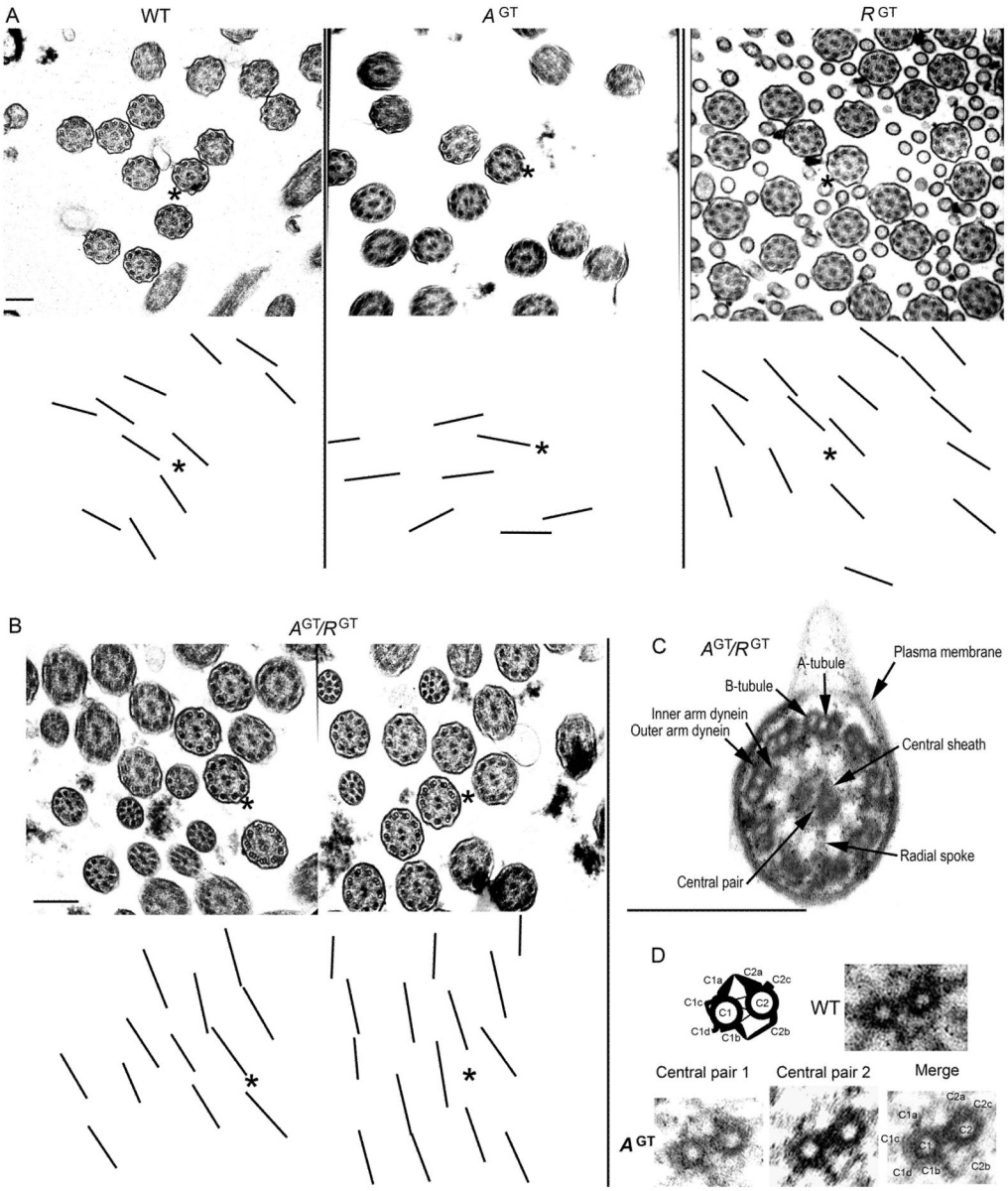

Figure 6. Ciliary alignment and axonemal ultrastructure are intact in mice that lack ASP and ROPN1

Trachea from wild type (WT), *Asp*^{GT} (A^{GT}), *Ropn1*^{GT} (R^{GT}), and *Asp*^{GT}/*Ropn1*^{GT} (A^{GT}/R^{GT}) mice were harvested and sectioned into rings prior to fixation and preparation for transmission electron microscopy (see Materials and Methods for details). In A and B, to assess whether cilia lacking ASP and/or ROPN1 were disoriented, a layer was created over the EM image (in Photoshop), and lines were drawn through the central pair of each axoneme. The layer was then offset so that central pairs would be visible in the presented images. Asterisks in corresponding upper and lower panels provide orientation. In C, a close up of an *Asp*^{GT}/*Ropn1*^{GT} (A^{GT}/R^{GT}) cilium showing that major ciliary structural components (as labeled in the figure) are intact in the absence of ASP and ROPN1.
In D, a diagram and an image of a wild type central pair apparatus (upper panel) and images of central pair apparatuses from flagellar axonemes that lack ASP [A^{GT} (lower panels), shows two raw axonemal images (left), and a merged image of the two axonemes with

central pair projections labeled (right, merge performed in Photoshop)]. Scale bars are 250 nm.

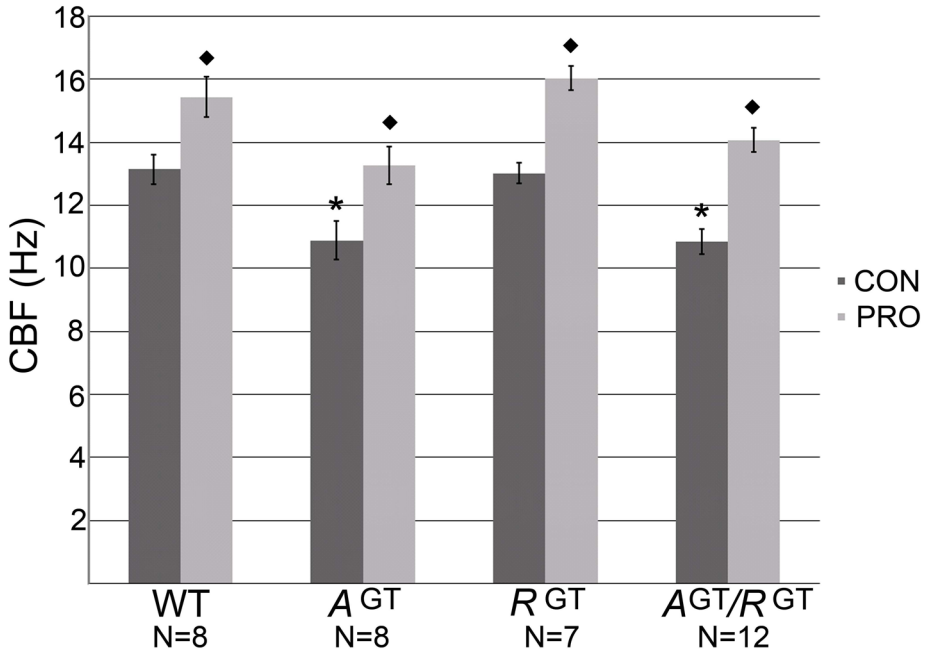

Figure 7. Basal ciliary motility is impaired by lack of ASP expression, while ROPN1 expression has no effect on motility

Trachea were harvested from wild type (WT), *Asp*^{GT} (*A*^{GT}), *Ropn1*^{GT} (*R*^{GT}), and *Asp*^{GT}/*Ropn1*^{GT} (*A*^{GT}/*R*^{GT}) mice, placed in serum-free M199 medium and sectioned into rings. Basal cilia beat frequency (CBF) of tracheal cilia was measured using the Sisson-Ammons Video Analysis (SAVA) system (CON bars). Rings were then stimulated with procaterol, (1 μM final concentration, PRO bars). N=8, 8, 7 and 12 animals respectively, as indicated on graph. * indicates significant decrease from WT CBF. ◆ indicates significant stimulation with procaterol. Error bars are standard error. Significance determined by ANOVA.

Table I

Male fertility parameters

Fertility is impaired in *Ropn1*^{GT} and *Asp*^{GT}/*Ropn1*^{GT} mice, but not *Asp*^{GT} mice. Motility of sperm from wild type, *Asp*^{GT}, *Ropn1*^{GT}, or *Asp*^{GT}/*Ropn1*^{GT} mice was assessed by trained observers. To determine fertility, male mice were housed with wild type female mice for a minimum of 5 weeks. N=10 for each line, ± indicates standard error.

	Sperm motility	% Fertile	Avg litter size[b]
Wild type	Vigorous	100	7.10 ± 0.71
***Asp*^{GT}**	Vigorous	100	6.88 ± 0.55
***Ropn1*^{GT}**	Variable[a]	40	3.75 ± 1.75
***Asp*^{GT}/*Ropn1*^{GT}**	Immotile	0	NA

[a] See Results for detail.

[b] Average litter size excludes infertile mice that produced no pups

Table II

Ciliary alignment (as measured by % standard deviation of central pair angles).

Ciliary alignment. Alignment of cilia in all mutant mouse lines (*Asp*^{GT}, *Ropn1*^{GT}, and *Asp*^{GT}/*Ropn1*^{GT}) is normal. As per clinical guidelines for identification of ciliary disorientation in the diagnosis of primary ciliary dyskinesia (laid out in Bush et al. 1998), at least 50 cilia from each line were examined (five separate fields of view that contained at least 10 cross-sectioned cilia with good central pair resolution) for ciliary orientation. Lines were drawn through each central pair in the field, and the standard deviation of the angles of these lines was calculated (number in parentheses is the number of cilia measured in the field), then averaged. ± indicates standard deviation.

	Wild type	***Asp*^{GT}**	***Ropn1*^{GT}**	***Asp*^{GT}/*Ropn1*^{GT}**
Field 1	13.1 (11)	12.1 (15)	12.1 (16)	10.5 (12)
Field 2	12.8 (17)	12.4 (18)	11.7 (19)	9.5 (17)
Field 3	11.8 (11)	11.8 (11)	7.6 (13)	8.7 (12)
Field 4	13.4 (10)	8.7 (13)	10.4 (12)	11 (13)
Field 5	8.5 (16)	13.3 (10)	8.2 (13)	11.2 (13)
Average	11.9±2 (65)	11.7±1.7 (67)	10±2 (73)	10.2±1.1 (67)